International Journal of Earth Sciences Knowledge and Applications
journal homepage: http://www.ijeska.com/index.php/ijeska

Research Article

e-ISSN: 2687-5993

Spatial Distribution of Aquifer Parameters from Petrographic, Vertical Electrical Sounding and Remote Sensing Data in Batang-Babete Locality, West-Cameroon

Sylvano Mouafo Saa[1], Jean Victor Kenfack[1]*, Njueya Kopa Adoua[1], Demanou Messe Malick Rosvelt[1], Kenzo-Tongnang Merlot Le-sage[1], Ngako Keuni[2], Kagou Dongmo Armand[1]

[1]Department of Earth Science, Faculty of Science, University of Dschang, PO Box.67, Dschang, Cameroon
[2]Department of Physics, Faculty of Sciences, University of Dschang, PO Box.67, Dschang, Cameroon

INFORMATION

Article history
Received 13 April 2021
Revised 13 January 2022
Accepted 14 January 2022

Keywords
Batang-Babete
Petrography
Geophysics
Remote sensing
Aquifer

Contact
*Jean Victor Kenfack
jvkenfi@yahoo.fr
victor.kenfack@univ-dschang.org

ABSTRACT

The aim of this work is to determine, using petrographic, geophysical and remote sensing studies, the spatial distribution of aquifers in the locality of Batang-Babete. The petrographic study reveals the existence of volcanic rocks (olivine basalt) throughout the study area. 1D inversion of Vertical Electrical Sounding (VES) using the Schlumberger type device highlights a multilayer aquifer system characterized by 13 types of anomalies: KH, HKH, KQ, QH, H, HK, AH, A, Q, AKH, K, KQH, KHKH, KHKH and HKH. The resistivity values given by VES and aquifer layer thicknesses have enabled spatial distribution of hydraulic parameters, parameters in front of conditioning the installation of water supply. The visible surface lineaments from Shuttle Radar Telecommunication Mission (SRTM) images reflect poor drainage in the study area. However, it follows from these lineaments two major directions which would correspond to the work of local tectonics N0-10° E and N160-170° E.

1. Introduction

Water is an essential issue for the next generation (Morel, 2007). However, water resources are becoming insufficient in the face of population growth**.** In Cameroon, the water supply structures installed by the village hydraulic program quickly find themselves unproductive when we know that the productivity of a water supply structure depends on the choice of its site. This choice involves mastering the aquifer system, in particular its depth, its flow, etc. In rural and peri-urban areas, the supply of good quality water remains very limited and people are fighting as best as they can to acquire water by obtaining supplies from streams, rivers and especially wells (Desruelle, 2009) although the quality of these waters remains to be deplored.

The locality of Batang which is part of the Highlands of West Cameroon (HTOC) has been facing for several years the problem of water supply in quantity and in quality. The population has recourse to wells although they present water whose quality remains to be deplored. The rare boreholes set up by the village hydraulic program are nowadays unproductive. This could be due to the ignorance of the aquifer system.

Evaluating the quantity of water available is essential for the development and management of water resources, be it drinkable water for populations, agricultural, industrial or energy production (UNESCO, 1997). It is therefore imperative to replenish the groundwater stock with a view of good management of resources to meet the needs of the population. This management therefore requires knowledge of the groundwater potential which can be achieved through

petrographic, geophysical and coupled remote sensing studies. These methods are of great interest so far as they allow the identification of the hydrogeological nature of the environment and the location of the water tables in depth.

This work was carried out in the locality of Batang using the methods of Desruelle (2009) and Kanohin et al. (2012) respectively in Mali and Ivory Coast, who have shown that the coupling of remote sensing and the electrical method prove to be very effective in locating and estimating the depth of aquifers with the view of establishing a quality map of the potential areas for drilling, helping to have a good estimate of the depths of the aquifers in the region.

The study area located in the locality of Batang is located between 5°36'0 " and 5° 37' 0" north latitude and 10° 15' 00" and 10 ° 16'30 " east longitude (INC, 2013).

The geomorphology is a characteristic of that of volcanic regions with elongated interfluves, slopes with steep slopes and U-shaped valleys. Altitudes vary in the area from 1316 to 1432 m.

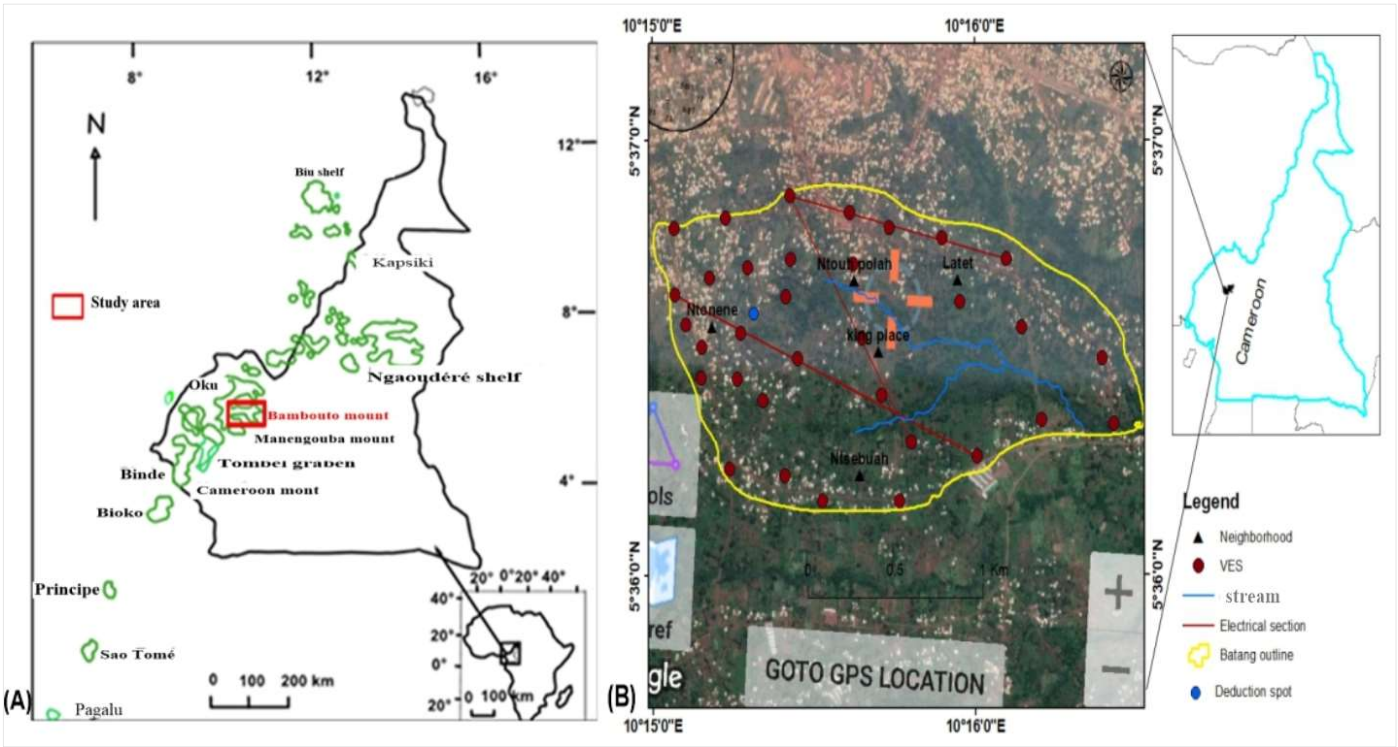

Fig. 1. localization (A) in Cameroon Volcanic Line (Deruelle et al., 2007) (B) Goto GPS localization

2. Geological and Hydrogeological Context

The study area is located on the eastern slope of the Bamboutos Mountain, in the HTOC (Yemmafouo et al. 2011). These mountains are part of the Cameroon Volcanic Line (CVL).

The Cameroon Volcanic Line is an N30°E alignment of anorogenic plutonic complexes and oceanic and continental volcanic massifs which extend from the Gulf of Guinea to Lake Chad (Fig. 1A). The CVL is oblique on the Cameroon center shear on which the Adamawa volcanic plateau is located. The CVL includes around sixty anorogenic complexes composed of various plutonic rocks (granite, syenite, diorite, gabbro), of mantle origin and alkaline to hyperalkaline affinity, sometimes associated with volcanism. They settle in the Upper Cretaceous (73 Ma) in the Middle Eocene (40 Ma). The oceanic and continental volcanic massifs are also alkaline. Volcanism begins around 44 Ma and continues sporadically until today (Vicat, 1998).

The study area has not yet been the subject of any published hydrogeological study. However, certain hydrogeological studies carried out along the Cameroon line (Nono et al., 2008; 2009; Mouafo 2010; Njueya et al., 2016), mention a surface aquifer system generally of the bilayer type. This aquifer system would include: (1) a regolith aquifer resting above a cracked basalt basement aquifer; (2) a regolith aquifer followed by pyroclast resting on more or less fractured basalts. Whatever the structuring model, the aquifers developed on pyroclast (mainly pozzolan) are more productive than those of fractured regolith and basalts (Nono et al., 2008, 2009; Mouafo, 2010; Masso, 2012; Njueya et al., 2016).

3. Data and methods

3.1. Data

The work consisted of finding outcrop formations and making macroscopic observations and descriptions throughout the study area. Only one petrographic type was observed during the field campaign: the sub aphyric basalt presenting minerals. The outcrop mode is in block with predominantly the weathering patina which recalls a chaotic

landscape resulting from weathering under the action of water. A detailed geological map was produced after microscopic observations at the Laboratory. At the right of each vertical electrical sounding point, the surface layers of soil were explored through a manual terrier to adjust the interpretations on the deep layers.

With regard to remote sensing data, in the field hydrogeological lineaments are materialized by the alignment of the large hundred-year-old trees and also by the route of the water system. The set (rock sample point, burrow point or vertical electrical sounding point) was recorded in Fig. 1B.

3.2. Methods

3.2.1 Petrographic method

The petrographic study consisted in locating the studied area on a geological background, carrying out a descent on the ground in order to sample the geological material and check its spatial arrangement contributing to carry out the geological map of the locality. Finally, the rock samples made it possible to make thin sections to better support the careful study of the geological material present in the studied area.

3.2.2. Electrical method

The aim of electrical prospection in hydrogeology is to determine the distribution of resistivities in the sub-soil in order to detect areas of anomalies favorable for the establishment of a hydraulic structure. The principle of implementation of the electrical method is based on the injection of the electric current of intensity I into the ground through 2 electrodes A and B and the measure of the potential difference ΔV produced by ohmic effect between two reception electrodes M and N. The principle of superposition and reciprocity teaches that this potential difference ΔV is the same as that which would be observed between A and B if the current was sent to M and N. It operates as follows: once the center of the device (O) is fixed, the current (A and B) and potential (M and N) electrodes are planted in the ground so that the potential electrodes are pointed between the current electrodes. Each electrode must be symmetrical to its counterpart relative to the center of the device. Then we move them away gradually, respecting the same symmetry. The electrodes M and N known as potential difference ΔV remain fixed for a series of readings and they are discarded for other series of data (declutching) while respecting the relation MN <AB/5 to avoid the phenomenon of running electrical outlets. During the field campaign 33 VES were done in the basaltic rock and the data collected subjected to computer processing using excel, ArcGIS, Jointem and res2dinv software.

The starting model of an iterative inversion process is most often homogeneous, with resistivity equal to the average of the apparent resistivities measured or even equal to the resistivity of an area recognized as not being part of the target sought (Marescot, 2004). The reverse operation of the direct problem is solved to go back to the unknown characteristics of the terrain from the measured responses. It is based on the data measured on the apparent ground, to find the parameters of the ground describing the subsoil in a plausible way and explaining well the measured data (Marescot, 2008). After treatment (inversion) a vertical section in calculated electrical resistivities is obtained and serves to highlight the geometry of geological bodies with contrasting electrical characteristics (Hacini, 2006).

1D inversion made it possible to group Vertical Electrical Soundings (VES) into thirteen major types of curves according to the principle of Koussoube et al. (2003). The JOINTEM modeling and inversion software made it possible to compare the calculated sounding curve with that measured and thus to modify the parameters of the model (thickness and resistivity of the different layers) in order to approximate the measured curve. The 1D inversion is only done at a single sampling point. Just like 1D inversions, 2D inversion software also allows you to compare the calculated sounding curve to the measured one and thus modify the parameters of the model (thickness and resistivity of the different layers) in order to get closer to the measured curve. This implementation makes it possible to obtain, after treatment (inversion), a vertical section in electrical resistivities calculated from the measurement of the apparent electrical resistivities using a multi-electrode device. Unlike the 1D inversion, the 2D inversion is done with several survey points aligned along a profile. The main objective is to highlight along the profile, the geometry of geological bodies with contrasting electrical characteristics, therefore the structure of the subsoil.

3.2.3. Hydraulic parameters

This is to build on the empirical relationship of Heigold et al. (1979) to calculate the hydraulic conductivity (K) of Prely realized 1D inversion cuts Attwa et al. (2014):

$$K = 386,4\rho^{-0.9328} \quad (1)$$

To determine the hydraulic conductivity of the aquifer, Equations where designs. The resistivity of the aquifer layer in Ω.m and K in m/day. It will still be a question of identifying Dar-Zarrouk's parameters of longitudinal conductance (S) and transverse resistance (Rt) following Obiora's approach (Obiora et al., 2018):

$$S = h/\rho \quad (2)$$

$$Rt = \rho.h \quad (3)$$

With h the thickness of the aquifer layer. And h has respect for unite Ω.m and m. S speaks in Ω^{-1} and Rt gives itself in $\Omega.m^2$.

According to the empirical relationship between Niwas and Singhal (1981):

$$K = Kt/h \quad (4)$$

Where Kt designs the transmissivity. Equation 4 so we can deduce Kt:

$$Kt = K.h \quad (5)$$

Kt gives in m^2/day.

3.2.4. Remote sensing method

Lineaments are lines resulting from morpho-structural alignments, alignments of natural trees, and the arrangement of branches of the hydrographic network or the straightness of geomorphological contours. The SRTM of Mbouda made it possible to highlight the lineaments visible on the surface, this is using the georeferencing software ArcGIS 10.2. These lineaments correspond on the ground to the righteousness of the geomorphological contours and to the layout of the hydrographic network.

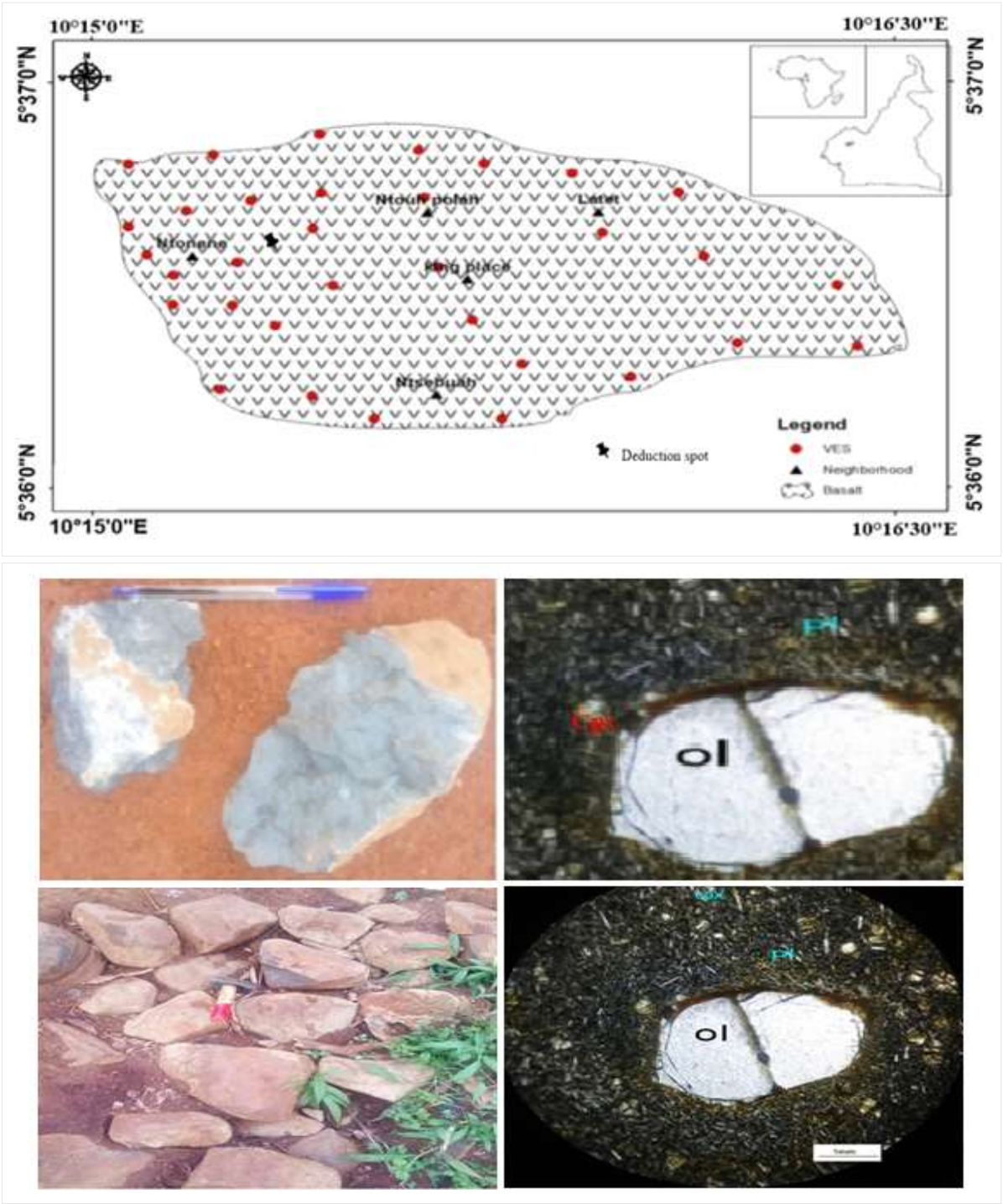

Fig. 2. Petrographic type of study area (A) spatial distribution of the rock (B) field sample (C) microscopic observation of the thin section (D) outcropping of the rock (E) microscopic observation of the thin section

This work required the use of SRTM and the geological map to manually generate the hydrogeological lineaments. It begins with the choice of the SRTM of the study area: this consists in determining the radar image of the studied area which allows better appreciation and comparisons between the different structures generated by image processing and those observed in the field. Here after georeferencing, the choice was made on the SRTM sheet N005E010, the

extraction of the SRTM from the study area of the sheet N005E010 and Digitalization according to the principle stipulates that the rectilinear portions of watercourses always correspond to old fracture lines and also following the alignment of natural vegetation. This consists of digitizing the different stream lines and that of the alignments of vegetation. The map of future water points is obtained after superimposing the lineaments layer on that of the Vertical Electrical Soundings, the hydrographic network and the piezometric level.

4. Results and Interpretations

4.1. Petrographic studies

Field observations made it possible to identify and map the geological formations that outcrop in the studied area (Figs. 2A, B, D). This revealed the presence of only one petrographic type: basalts. They are exposed in the block study area with a yellowish weathering patina. These basalts have a dark color, mega crystals visible to the naked eye which under the microscope are olivine. The rock therefore has a sub aphyric texture.

Under a microscope, the rock presents a porphyritic microstructure (Figs. 2C, E) composed of olivine phenocrysts in a microlitic matrix containing small brown crystals of clinopyroxene, small rod crystals of plagioclase and oxides. Olivine (35-40%) is in the form of xenomorphic phenocrysts but there are still medium-sized crystals and also microcrystals. The olivine crystals are irregularly shaped and contained in a microlitic paste of plagioclase (present in the form of baguette microcrystals in the rock matrix between 25-30%) and clinopyroxene (present in the rock matrix in the form of microcrystals. They appear as brownish automorphic crystals and have cleavages almost sometimes invisible on other crystals due to the phenomenon of alteration). The olivine crystals have a strong relief, with characteristic cracks and a very marked start of deterioration at their edges. An inclusion of oxide is observed in the central phenocryst. It is the olivine phenocrysts that give the rock the porphyritic microstructure. Accessory minerals (<10%): are mainly oxides. Most of them arise from the destabilization of plagioclase feldspar. Opaque minerals are also encountered along the cracks of olivine.

4.1. Vertical Electrical Sounding

4.1.1. 1D inversion

The typology of sounding curves makes it possible to distinguish: KH type curves (Fig. 3A) represented by 7 stations (VESs: 1, 23, 25, 32, 3, 8, 17), HKH type curves (W) (Fig. 3B) represented by 04 stations (VESs: 2, 22, 28, 30), KQ type curves (Fig. 3C) is represented by 03 stations (VESs: 7, 14, 26), QH type curves (Fig. 3D) represented by 04 stations (VESs: 9, 12, 20, 21), H type curves (Fig. 3E) represented by 05 stations (VESs: 10, 33, 4, 6, 29), HK type curves (Fig. 3F) represented by 01 station (VES11), AH type curves (Fig. 3H) represented by 01 station (VES13), A (Fig. 3G) represented by 01 station (VES15), Q (Fig. 3J) represented by 02 stations (VES: 16, 27), AKH type curves (Fig. 3I) represented by 01 station (VES18), K type curves (Fig. 3M) represented by 01 station (VES19), KQH type curves (Fig. 3L) represented by 01 station (VES24) and KHKH type curves (KW) (Fig. 3K) represented by 01 station (VES31).

The KH curves or bell curve followed by a boat bottom are characteristic of the areas where there is an alternation of four volumes of land including two conductive land alternating with two resistant land respectively. The bottom of the boat would be the appropriate position for the location of the water table because**;** this level indicates a drop in resistivity probably a fracture containing a fluid which could be water. It would be an aquifer with one layer because the funds of boat of the various drillings extend in single layers. These curves present roofs of aquifers located in the third layer which is the conducting layer for the VES1, VES8, VES5, VES17, and VES23. The depths of the aquifer roofs given by the curve are respectively 40-50 m; 32-38 m; 40-52 m; 10-15 m; 40-50 m this being justified by Boudoukha (2008) who gives the depth of aquifer roofs the abscissa of the bottom of the boat for abscissas of the bottom of the boat identified less than 100 m. According to the empirical relationship of Barker (z = 0.19AB) these aquifer roofs are rather at depths 15.2-19 m; 12.16-14.44 m; 15.2-19.76 m; 3.8-5.7 m and 15.2-19 m respectively. The aquifer roofs would be located in the fourth layer for VES3, VES25, and VES32 at depths of 30-40 m, 30-52 m, 40-50 m respectively according to the theory stated by Boudoukha (2008).

But between 11.4-15.2 m; 11.4-19.76m and 15.2-19m respectively based on Barker's relationship. The VES grouped in the KH typology presents 04 layers for the VES1, VES8, VES23 and VES5. VES17, VES32 and VES3 have 05 layers while VES25 have 07 layers. For four-layer VES, we note that layers 03 would be the conductive layers with respective resistivities of 68.62 Ω.m, 11.72 Ω.m, 24.36 Ω.m and 68.62 Ω.m. In view of their resistivity values, these layers would be hydrated clays which would mark the reaching of the aquifer level. For VES with 05 layers, the conductive layer would be the fourth layer for VES32 and VES17 with the respective values 32.5 Ω.m and 134.18 Ω.m. The fourth layer for VES32 would also represent hydrated clay while that of VES17 would be an altered formation and necessarily a laterite having conductivity due to the presence of an interstitial or otherness layer. VES25 carries a fifth conductive layer of resistivity 64.04 Ω.m which according to the abacus of Hoareau (2009) is also hydrated clay.

HKH curve or curves with a bell separating two boat bottoms are characterized by three resistant terrains alternating with two conductive terrains. As in all types of curves with a bottom of the boat, the conductive layers which present the bottom of the boat would probably be fractured and the presence of fluid in these fractures causes the resistivity to drop. This fluid would probably be water which marks the reaching of the aquifer level. These curves show aquifer roofs in the second and fourth layer for VES22, VES28, VES30 for depths of 3-3.8 m and 38-50 m respectively; 4 m and 48-60 m; 2 m and 48-60 m and in the second and fifth layers for VES2 with an aquifer roof located at 6 m and 38-48 m. These depth values would be identical if one applied Boudoukha's theory (Boudoukha, 2008) but according to Barker the depths of aquifer roofs would rather be for VES22, VES28, VES30 and VES2 respectively 1.14-1.44 m and 14.44 -19 m; 1.52 m and 18.24-22.8 m; 0.76 m and 18.24-22.8 m. In this type of curve, the aquifer level extends in two different layers; this indicates the presence of a superimposed multilayer aquifer

attesting that the resistant layer separating the two conductive layers would be an impermeable layer and probably fluid clay.

The VES2 has an electrical cut with 06 layers including two conductive layers for four resistant layers. These conductive layers have resistivity values of 649.16 Ω.m and 192.71 Ω.m respectively. These resistivity values show that these two layers would be altered formations and more precisely laterites carrying layers of otherness. VES2, VES28 and VES30 are five layers and have two conductive layers for three resistant layers. These conductive layers are for all these VES the second and fourth layer. For VES22 these second and fourth layers would be laterite and clay respectively.

For VES28 layer two would designate a fractured formation (fractured basalt) and layer four would designate a laterite. For VES30, layer two would be laterite and layer four would be clay.

The QH type curves shows a sharp decrease in staircase which is followed by a bottom of the boat. This type of curve is characterized by two consecutive resistant layers but of different nature which is followed by two other layers, one conductor marking the bottom of the boat and the other resistant. The electrical sounding curves for this type show the aquifer roofs in the third layer (conductive layer) for VES12, VES20, VES21 this, at depths of 40-50 m; 38-50 m; 40-50 m; in the fourth layer by application of Boudoukha theory (Boudoukha, 2008). These values would be 15 m; 2-19 m; 14.44-19 m; 15.2-19 m respectively for VES12, VES20, VES21 and VES9. The aquifer system for this type of curve would therefore be that of a layer. The QH type VES (VES12, VES20 and VES21) all have 04 layers with the exception of VES9. These 04-layer VES all have their third conductive layers. These conductive layers have resistivity respectively 21.31 Ω.m, 19.19 Ω.m and 188.71 Ω.m. By comparing these values with those of the abacus of Hoareau (2009) we see that these third layers are hydrated clays for VES12 and VES20 which marks the presence of the water table. This third layer for VES21 would be laterite carrying an interstitial or other sheet. The electrical section of the VES9 has 05 layers and the conductive layer is the fourth layer. It has a resistivity of 16.35 Ω.m characteristic of hydrated clays.

The H curves or curve at the bottom of the boat are characterized by a conductive layer sandwiched by two resistant layers. The conductive layer is probably fractured. These curves show the aquifer roofs in the second layer, for VES4, VES6, VES10, VES33 whose depths are respectively 3 m, 5 m, 18 m and a flat bottom between 3-6 m; and the roof in the fourth layer for the VES29 at a depth of 20-25 m (almost flat bottom) these values are equal to those obtained according to the Boudoukha theory (Boudoukha, 2008) but according to Barker these depths would be 1.14 m; 1.19 m; 6.84 m; 1.14-2.28 m and 7.6-9.5 m. These curves also designate single-layer aquifers. VES6 and VES10 are three-layer and have a second conductive layer. VES4, VES33 wear 04 layers and VES29 wear 06 layers. The VES6 and VES10 have been made in a battleship zone, they carry second layers which have resistivity's of 214.14 Ω.m and 410.10 Ω.m respectively.

These would be laterite layers carrying regolith layers. VES4 and VES33 have the second conductive layer with resistivity of 275.45 Ω.m and 501.29 Ω.m respectively. For VES4, this value marks the presence of an altered formation which would be a laterite, as for VES33 it indicates the presence of a fractured formation which would be an altered basalt. The VES29 has the fourth conductive layer. It has a resistivity of 78.42 Ω.m which bring it closer to hydrated clay.

The curves HK, AH, AKH, KQH respectively designate curves at the bottom of the boat followed by a bell, with growth in steps followed by a bottom of the boat, with growth in steps followed by a bell and a bottom of boat and a bell followed by a decay and a boat bottom. These layers all have single-layer aquifers. These curves are designated respectively by VES11, VES13, VES18, VES24 and have layers 02, 03, 03 and 05 at respective aquifer roofs at depths of 10 m, 80 m, 40-50 m, 70-80 m values read on curves and in accordance with Boudoukha theory (Boudoukha, 2008) and would be according to Barker 3.8 m; 30.4 m; 15.2-19 m; 26.6-30.4 m. The HQ (VES11), AH (VES13), AKH (VES18), and KQH (VES24) curves show a single bottom of the boat.

The cut of VES11 presents as a conductive layer the second with resistivity 207.04 Ω.m which would be a laterite. The cut of VES13 presents its third as being conductive, it would also be a laterite just like the conductive layer of VES18 while that of VES24 would be clay.

The curves type KHKH or KW or curve with two boat bottoms and two bells characterize a multilayer aquifer and are designated in the field by VES9 and VES31. VES31 has conductive layers in positions 03 and 05 at depths of 8 m and 32 m identical to the values obtained after using Boudoukha theory (Boudoukha, 2008) but would be 1.14 m and 12.16 m according to Barker. The KHKH curve represented by the VES31 presents an electrical section with 06 layers, including two conductive layers (layers three and five) having a resistivity value of 84.61 Ω.m and 77.14 Ω.m and both denote hydrated clays.

The Q curves or descending staircase curves are characterized by a monotonous curve with resistivities which decrease progressively from the first layer to the last. These curves show the last layers (source rock) with very low resistivity values compared to the other layers. This would designate an incomplete survey (Njueya et al., 2016) but still shows that the aquifer level has been reached, which means that the aquifer in this type of curve is located in the source rock. The source rock here would be the fractured level in which fluids (water) circulate. These types of curves would also designate a single-layer aquifer.

Type K curves or bell curves are characteristics of a medium with a resistant layer surrounded by two conductive layers. Like the Q-type curves, they have a final conductive layer and therefore fractured layer (parent rock). This type of curve is designated by VES19 and according to Boudoukha theory (Boudoukha, 2008). It is still possible for this type of curve to estimate the depth of the aquifer more precisely from its wall. For VES19 the wall of the aquifer would be 16 m according to Boudoukha theory (Boudoukha, 2008).

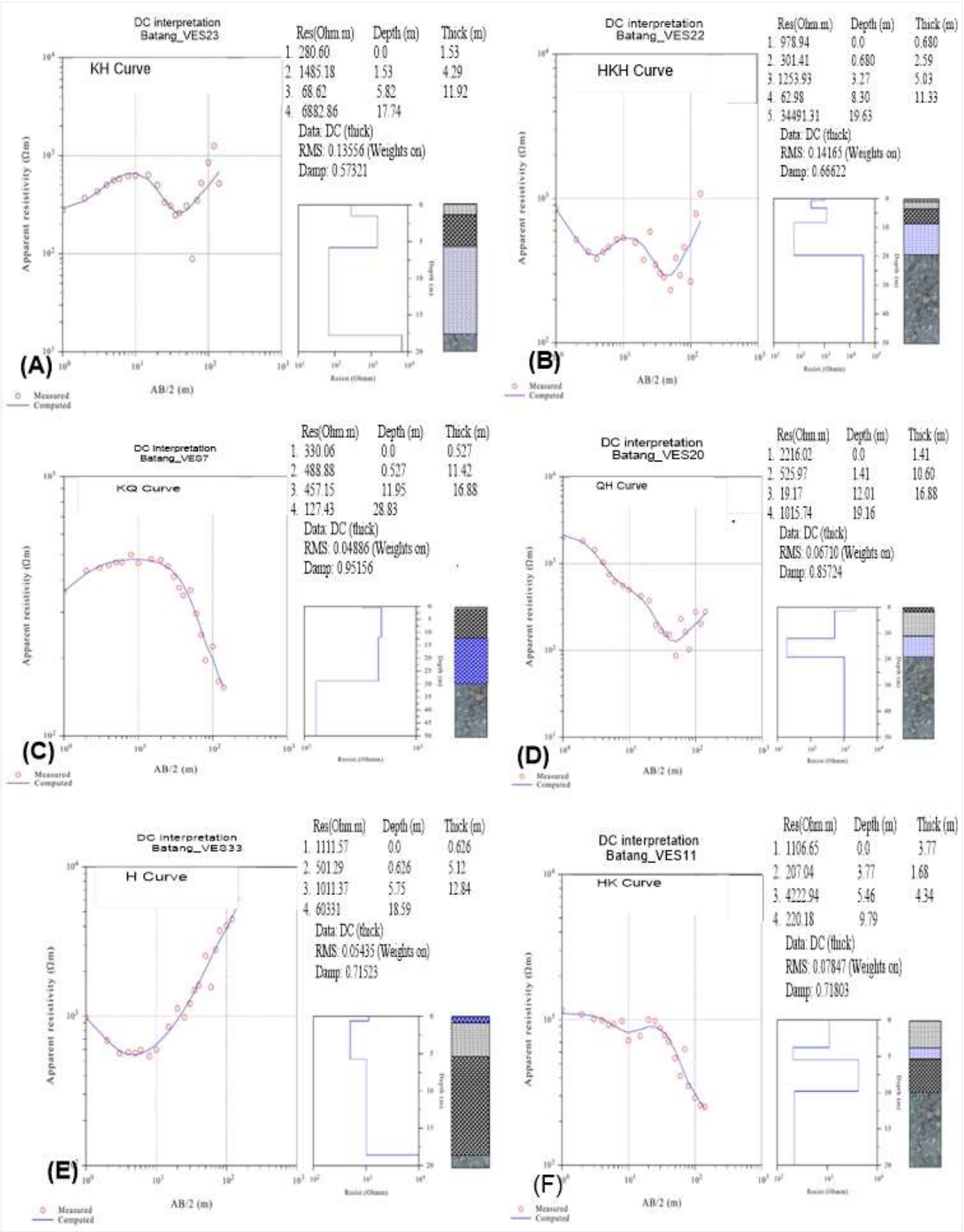
DC interpretation
Batang_VES23
KH Curve
Res(Ohm.m) Depth (m) Thick (m)
1. 280.60 0.0 1.53
2. 1485.18 1.53 4.29
3. 68.62 5.82 11.92
4. 6882.86 17.74
Data: DC (thick)
RMS: 0.13556 (Weights on)
Damp: 0.57321
(A)
DC interpretation
Batang_VES22
HKH Curve
Res(Ohm.m) Depth (m) Thick (m)
1. 978.94 0.0 0.680
2. 301.41 0.680 2.59
3. 1253.93 3.27 5.03
4. 62.98 8.30 11.33
5. 34491.31 19.63
Data: DC (thick)
RMS: 0.14165 (Weights on)
Damp: 0.66622
(B)
DC interpretation
Batang_VES7
KQ Curve
Res(Ohm.m) Depth (m) Thick (m)
1. 330.06 0.0 0.527
2. 488.88 0.527 11.42
3. 457.15 11.95 16.88
4. 127.43 28.83
Data: DC (thick)
RMS: 0.04886 (Weights on)
Damp: 0.95156
(C)
DC interpretation
Batang_VES20
QH Curve
Res(Ohm.m) Depth (m) Thick (m)
1. 2216.02 0.0 1.41
2. 525.97 1.41 10.60
3. 19.17 12.01 16.88
4. 1015.74 19.16
Data: DC (thick)
RMS: 0.06710 (Weights on)
Damp: 0.85724
(D)
DC interpretation
Batang_VES33
H Curve
Res(Ohm.m) Depth (m) Thick (m)
1. 1111.57 0.0 0.626
2. 501.29 0.626 5.12
3. 1011.37 5.75 12.84
4. 60331 18.59
Data: DC (thick)
RMS: 0.05435 (Weights on)
Damp: 0.71523
(E)
DC interpretation
Batang_VES11
HK Curve
Res(Ohm.m) Depth (m) Thick (m)
1. 1106.65 0.0 3.77
2. 207.04 3.77 1.68
3. 4222.94 5.46 4.34
4. 220.18 9.79
Data: DC (thick)
RMS: 0.07847 (Weights on)
Damp: 0.71803
(F)
Apparent resistivity (Ωm)
AB/2 (m)
Measured
Computed

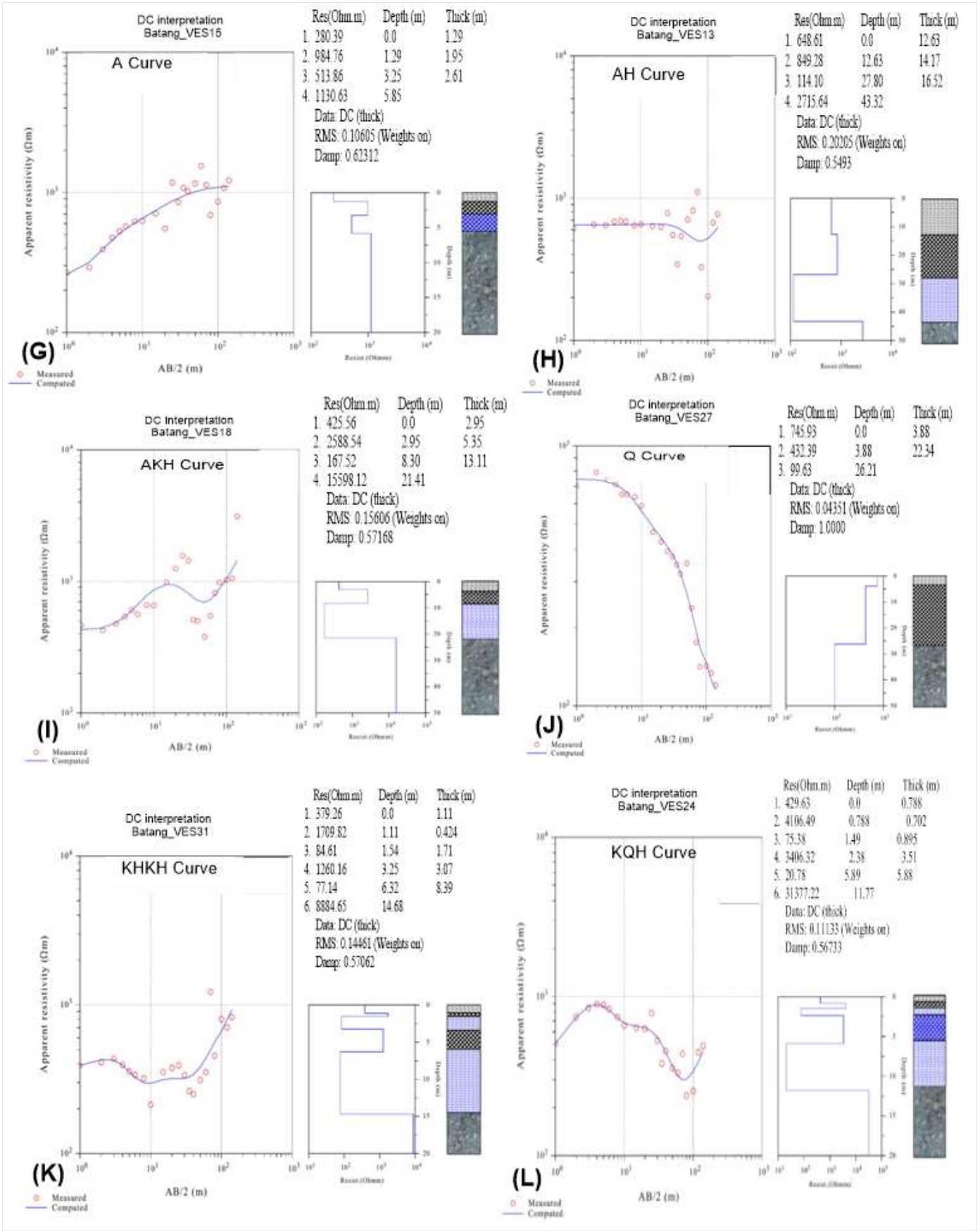
DC interpretation
Batang_VES15
A Curve
Res(Ohm.m) Depth (m) Thick (m)
1. 280.39 0.0 1.29
2. 984.76 1.29 1.95
3. 513.86 3.25 2.61
4. 1130.63 5.85
Data: DC (thick)
RMS: 0.10605 (Weights on)
Damp: 0.62312
Apparent resistivity (Ωm)
AB/2 (m)
Measured
Computed
(G)
DC interpretation
Batang_VES13
AH Curve
Res(Ohm.m) Depth (m) Thick (m)
1. 648.61 0.0 12.63
2. 849.28 12.63 14.17
3. 114.10 27.80 16.52
4. 2715.64 43.32
Data: DC (thick)
RMS: 0.20205 (Weights on)
Damp: 0.5493
Apparent resistivity (Ωm)
AB/2 (m)
Measured
Computed
(H)
DC Interpretation
Batang_VES18
AKH Curve
Res(Ohm.m) Depth (m) Thick (m)
1. 425.56 0.0 2.95
2. 2588.54 2.95 5.35
3. 167.52 8.30 13.11
4. 15598.12 21.41
Data: DC (thick)
RMS: 0.15606 (Weights on)
Damp: 0.57168
Apparent resistivity (Ωm)
AB/2 (m)
Measured
Computed
(I)
DC interpretation
Batang_VES27
Q Curve
Res(Ohm.m) Depth (m) Thick (m)
1. 745.93 0.0 3.88
2. 432.39 3.88 22.34
3. 99.63 26.21
Data: DC (thick)
RMS: 0.04351 (Weights on)
Damp: 1.0000
Apparent resistivity (Ωm)
AB/2 (m)
Measured
Computed
(J)
DC interpretation
Batang_VES31
KHKH Curve
Res(Ohm.m) Depth (m) Thick (m)
1. 379.26 0.0 1.11
2. 1709.82 1.11 0.424
3. 84.61 1.54 1.71
4. 1260.16 3.25 3.07
5. 77.14 6.32 8.39
6. 8884.65 14.68
Data: DC (thick)
RMS: 0.14461 (Weights on)
Damp: 0.57062
Apparent resistivity (Ωm)
AB/2 (m)
Measured
Computed
(K)
DC interpretation
Batang_VES24
KQH Curve
Res(Ohm.m) Depth (m) Thick (m)
1. 429.63 0.0 0.788
2. 4106.49 0.788 0.702
3. 75.38 1.49 0.895
4. 3406.32 2.38 3.51
5. 20.78 5.89 5.88
6. 31377.22 11.77
Data: DC (thick)
RMS: 0.11133 (Weights on)
Damp: 0.56733
Apparent resistivity (Ωm)
AB/2 (m)
Measured
Computed
(L)

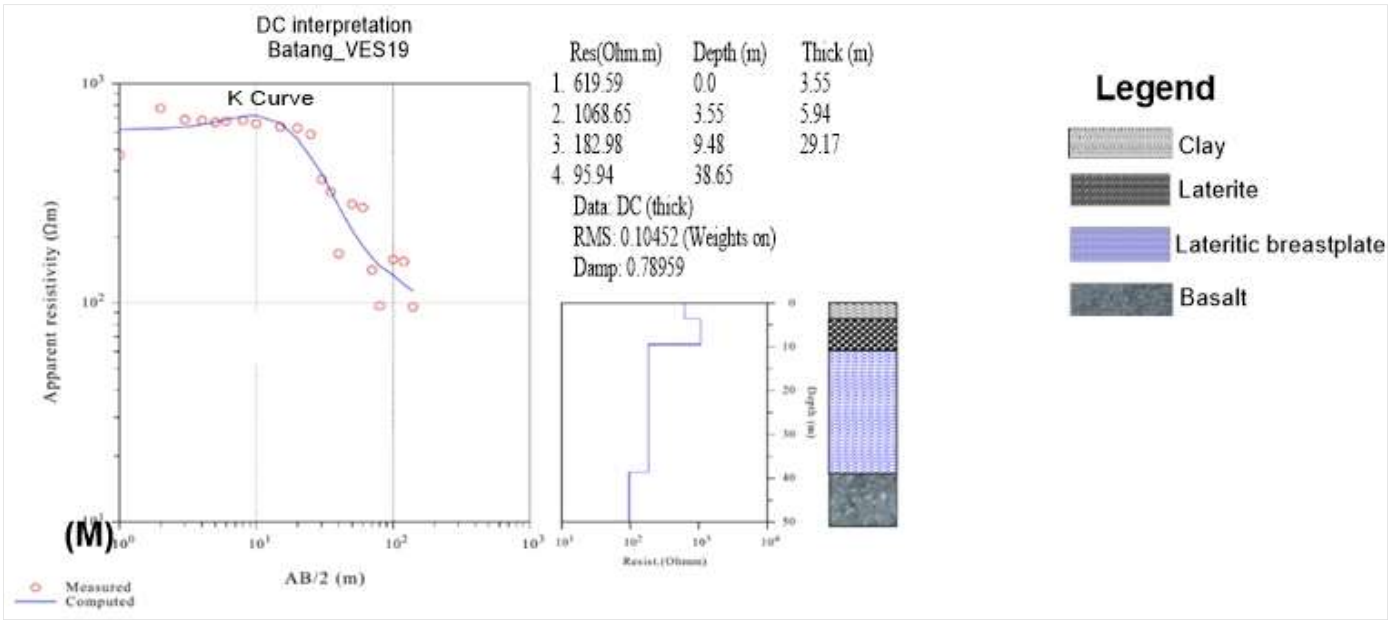

Fig. 3. Typical curves of electrical surveys in the study area

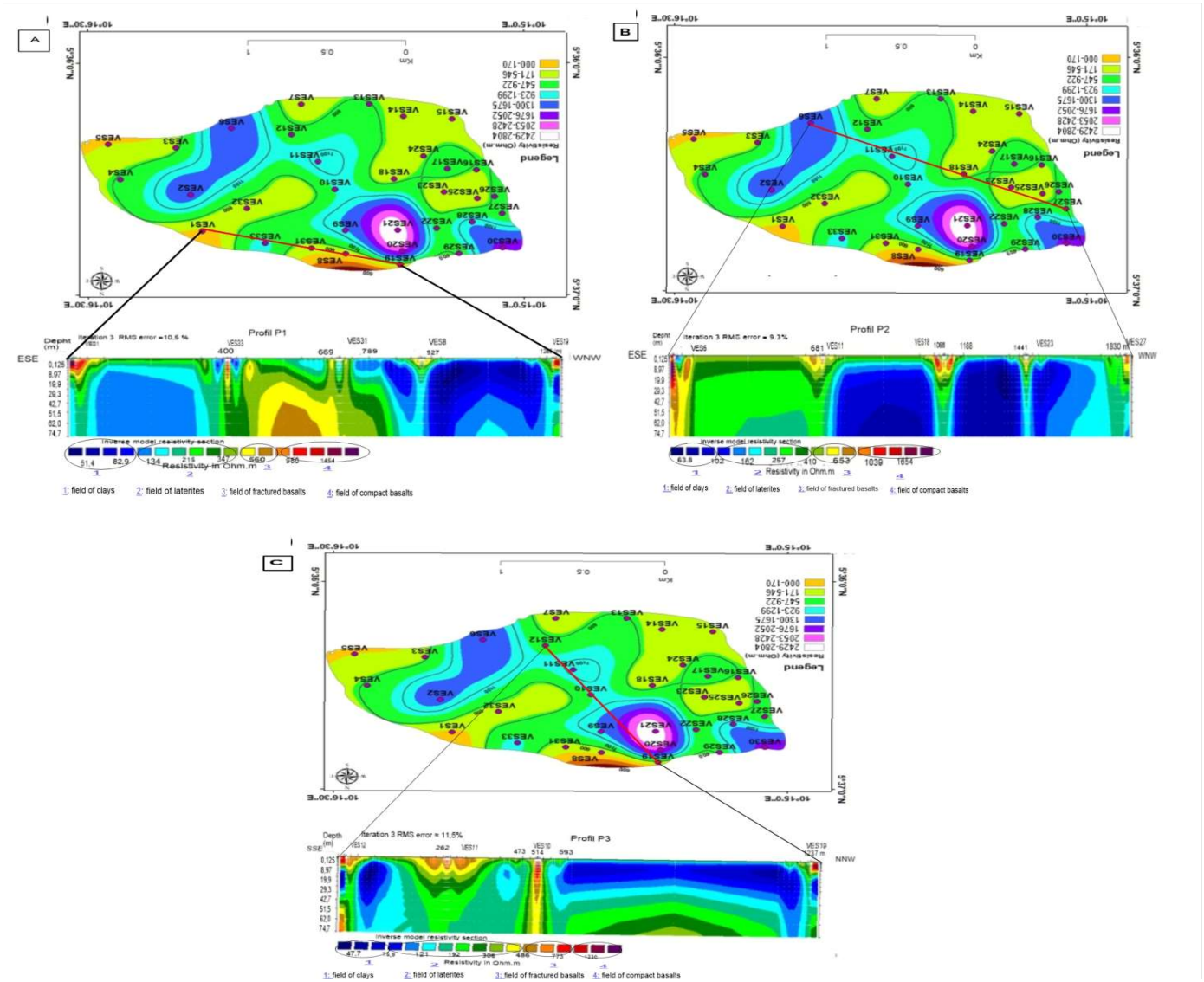

Fig. 4. 2D inversion; position of Profiles on the study area; (A) Profile P1, (B) Profile P2 and (C) profile P3

The P3 profile (Fig. 4C) has two major anomalies. In line with VES12, the first anomaly occurs in an elongated spindle and pierces up to 51.5 m deep for an almost punctual lateral spread on the scale of the profile. The roof of this anomaly is almost 4 m from the surface. This anomaly layer has a resistivity of 75.5 Ω.m and is trapped in a resistivity layer equal to 121Ω.m which according to Hoareau (2009) is hydrated clay**.** Between 593 m and 1237 m, we note the presence of a very deep spindle anomaly with two layers, one with resistivity of 121 Ω.m and the second with resistivity of 75.9 Ω.m. It would be a laterite layer carrying a Regolith or superficial aquifer level.

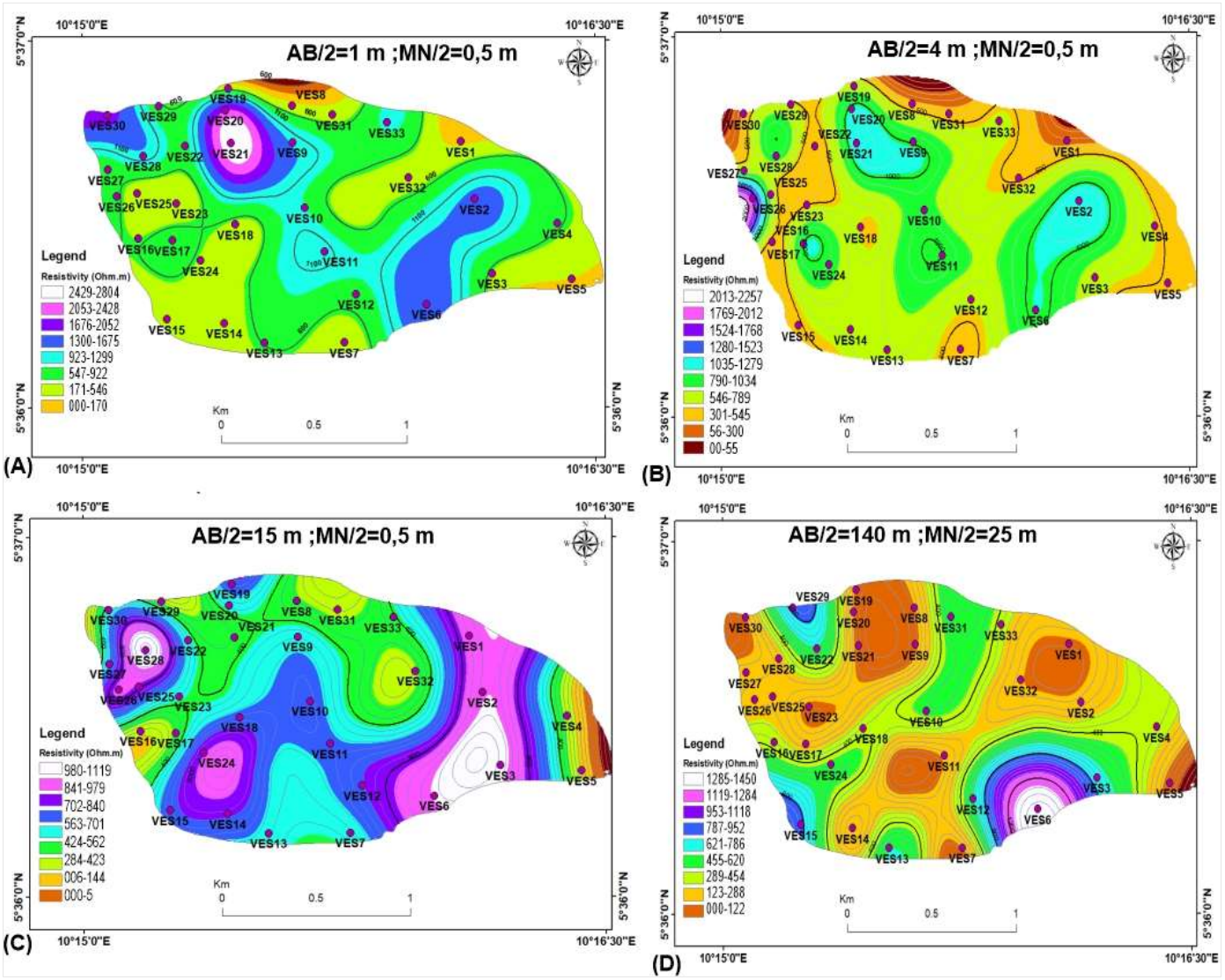

Fig. 5. Iso-resistivity maps

The P2 profile (Fig. 4B) presents, very large anomalies whose roofs are found almost 8 m from the surface and the walls at depths going beyond 74.7 m with resistivities between 106 Ω.m and 162 Ω.m. In view of these resistivity values, and according to Hoareau (2009), we would be dealing with a level of alteration which in our area of study would be laterites. These layers are therefore of the superficial type or regolith layers.

The P1 profile (Fig. 4A) presents 06 anomalies: the first between 0 to 488 m on the profile which has a strong lateral spread and a roof almost 14 m deep and its wall beyond 74.7 m. It therefore has a resistivity of 134 Ω.m. We also observe two points anomalies around 488 m with resistivities close to 134 Ω.m. Between 789 m and 927 m, we also observe quasi-point anomalies with the same resistivity value as that of the previous one. Between 927 m and 1.265 km, we observe an anomaly of very large thickness and very high horizontal spread. Its roof is almost 2 m deep and its wall varies over its entire extent (going in places to 30 m and goes beyond 74.7 m from the surface).

According to Hoareau (2009), these anomalies marked by 134 Ω.m resistivities are laterites and therefore mark sheets of regolith or superficial. The influence of the water table on the hydrographic network is reflected between VES10 and

VES19 and is marked by the presence of a very thick anomaly designating a free water table the water table is therefore at the origin of the waters of the hydrographic network.

4.2.3. The apparent iso-resistivity maps

The different iso-resistivity maps produced at different depths shows vertical and lateral heterogeneity. This variation is due to the multiplicity of the layers on the vertical plane. The interpretations of these maps are made using the charts of Marescot (2006) and Hoareau (2009) and relate to the resistivity intervals of 400-800 Ω.m which according to the charts for the basement areas would designate fractured formations fractured and which therefore have a great hydrogeological interest. Observations suggest that the iso-resistivities that mark changes in lateral resistivity are the depths of 1 m, 2 m, 3 m, 4 m, 10 m, 30 m, 60 m, 100 m, 140 m. According to the similarity existing between the different maps, the most representative is presented in Fig. 5.

Table 1. Summary of result of interpreted layer parameters from the study area

VES	Longitude (°)	latitude (°)	Layer No	Aquifer resistivity ρ (Ω.m)	Aquifer thickness h (m)	Hydraulic conductivity K (m/day)	Transverse resistance Rt (Ω.m²)	Longitudinal conductance S (1/Ω)	Transmissivity Kt (m²/day)
VES1	10.2684	5.6121	3	68.62	11.92	7.48	817.95	0.17	89.17
VES2	10.2691	5.6095	2	649.16	3.36	0.92	2181.18	0.01	3.09
			5	192.71	10.37	2.86	1998.40	0.05	29.61
VES3	10.2699	5.6061	4	134.18	13.82	4.00	1854.37	0.10	55.31
VES4	10.2731	5.6083	2	275.45	1.81	2.05	498.56	0.01	3.70
VES5	10.2738	5.6058	3	11.72	10.65	38.90	124.82	0.91	414.25
VES6	10.2501	5.6047	2	214.14	1.25	2.59	267.68	0.01	3.23
VES8	10.2603	5.6138	3	24.36	4.54	19.66	110.59	0.19	89.24
VES9	10.2602	5.6121	4	16.35	13.21	28.51	215.98	0.81	376.65
VES10	10.2608	5.6091	2	470.1	17.56	1.24	8254.96	0.04	21.82
VES11	10.2618	5.6071	2	207.04	1.68	2.67	347.83	0.01	4.49
VES12	10.2633	5.6051	3	21.31	8.46	22.27	180.28	0.40	188.39
VES13	10.2588	5.6030	3	114.1	16.52	4.66	1884.93	0.14	76.90
VES17	10.2544	5.6076	3	166.81	2.7	3.27	450.39	0.02	8.82
VES18	10.2574	5.6083	3	167.52	13.11	3.25	2196.19	0.08	42.65
VES20	10.2570	5.6107	3	19.17	7.15	24.58	137.07	0.37	175.74
VES21	10.2572	5.6120	3	188.71	15.87	2.91	2994.83	0.08	46.20
VES22	10.2550	5.6119	2	301.41	2.59	1.88	780.65	0.01	4.87
			4	62.98	11.33	8.10	713.56	0.18	91.82
VES23	10.2546	5.6093	3	68.62	11.92	7.48	817.95	0.17	89.17
VES24	10.2557	5.6067	3	75.38	0.89	6.85	67.09	0.01	6.10
			5	20.78	5.88	22.80	122.19	0.28	134.05
VES25	10.2526	5.6086	5	64.04	6.35	7.98	406.65	0.10	50.66
VES28	10.2529	5.6114	2	744.85	4.2	0.81	3128.37	0.01	3.40
			4	131.02	14.44	4.09	1891.93	0.11	59.09
VES29	10.2538	5.6138	2	73.42	4.64	7.02	340.67	0.06	32.59
			4	73.48	4.64	7.02	340.95	0.06	32.56
VES30	10.2512	5.6134	2	284.9	3.56	1.98	1014.24	0.01	7.06
			4	36.94	9.05	13.33	334.31	0.24	120.64
VES31	10.2621	5.6133	3	84.61	1.71	6.15	144.68	0.02	10.52
			5	77.14	8.36	6.71	644.89	0.11	56.07
VES32	10.2658	5.6105	4	32.5	7.18	15.02	233.35	0.22	107.85
VES33	10.2648	5.6129	2	501.29	5.12	1.17	2566.60	0.01	5.99

For the depth of 1 m (Fig. 5A), the VES9, VES21, VES20, VES22, VES28, VES30, VES6, VES11, VES2 would appear to be located on the healthy source rock (basalt) at resistivities >1000 Ω.m while that of VES3, VES4, VES32, VES8, VES31, VES19, VES18, VES14, VES12, VES24, VES16, VES29, VES33, VES17 with resistivities between 400-800 Ω.m would be in the basalt fractured formations. For resistivities between 80-400 Ω.m we note the VES1, VES5, VES15, VES23, VES25 located in environments corresponding to the formations altered more precisely laterites after the Marescot chart (Marescot, 2006).

For depths of 2 m, the VES7, VES15, VES3, VES4, VES32, VES33, VES31, VES8, VES14, VES17, VES18, VES23, VES24, VES22 and VES25 would be located in basalt fractured formations (400-800 Ω. m). At 4 m (Fig. 5B) deep, the resistivity range between 400-800 Ω.m carries the VES12, VES13, VES14, VES18, VES23, VES27, VES28, VES29 and VES33. At 25 to 30 m depth, the resistivity range of 400-800 Ω.m is occupied by the VES1, VES3, VES4, VES10, VES11, VES14, VES15, VES 25, VES 7, VES18, VES26, VES27 and VES33. At 60 m depth, the VES1, VES3, VES13 and VES33 occupies the domain of fractured rocks. At 100 m depth we have the VES6, VES15, VES26, VES29 and VES31 which occupy the domain of fractured rocks. At 140 m depth (Fig. 5D), the resistivity range of 400-800 Ω.m is occupied by the VES3, VES10, VES12, VES13, VES22, VES24 and the VES31. Any VES located in a fractured domain on an iso-resistivity map can only show an aquifer level if it is located on a hydrated fracture.

4.3. Hydraulic parameters

The values of hydraulic conductivity vary in the study area from 0.81 to 38.9 m/day (Table 1). Longitudinal conductance values range from 0.01 to 0.91 Ω^{-1}. In terms of the values of transmissivity, in the study area, the variation

ranges from the value 3.09 m2/day to the value of 414.28 m^2/day. The aquifer layers showing great hydraulic conductivity are the same ones that have high values of longitudinal conductance and also of transmissivity. These large values are listed on the aquifer layers of VES5, VES8, VES9, VES12, VES20, VES24, VES30 and VES32 and are located to the north, center and east of the study area. The different parameters calculated from resistivity's and thicknesses of the conductive layers of VESs are summarized in the table opposite.

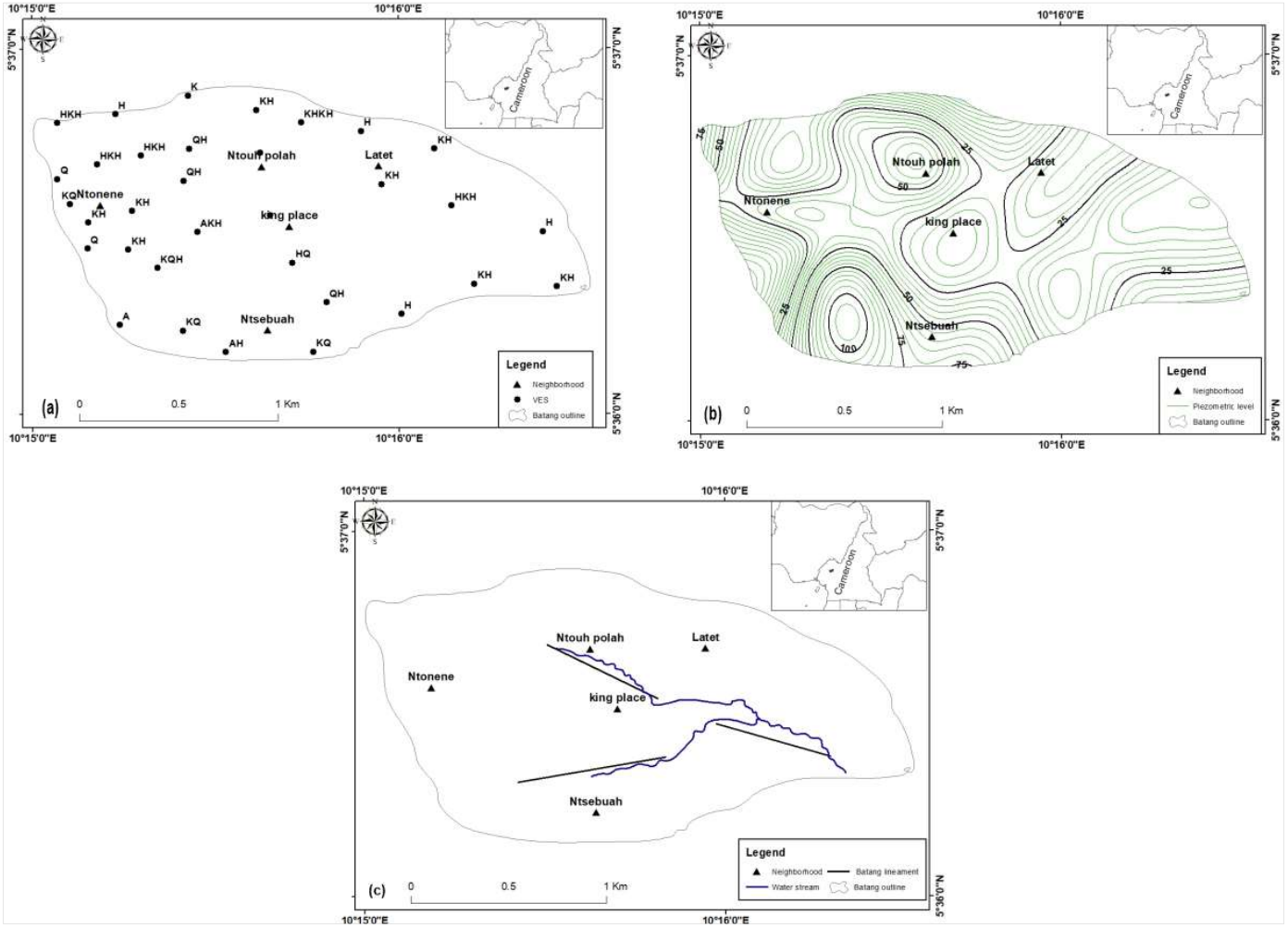

Fig. 6. a) VES spatial repartition, b) piezometric map and c) hydrology and lineament network

4.4. Lineaments from SRTM

The analysis made it possible to locate 03 lineaments which were reported on the map by a manual digitization process (Fig. 6). According to the observation of the rose window, the Batang area presents for major directions N0-10 ° E and N160-170 ° E. The major directions of the surface lineaments obtained by processing the SRTM of Mbouda are in descending order N70-80° E, N40-50° E, N30-40° E and the minor directions in ascending order are N130-140° E, N150-160° E and N0-10° E. With regard, these directions are almost in accordance with the results obtained by Njueya et al. (2012) in the Douala sedimentary basin, these major directions would correspond to those of the major accidents of the Pan-African chain from central Africa to Cameroon: the largest direction which is N70-80° E would correspond to that of Central Cameroon Shear Zone (CCSZ) but also that of the Sanaga Fault; the direction N30-40° E is identical to that of the volcanic line of Cameroon.

The major structural features and morpho-structures detected on the images therefore correspond to real accidents that affect the basement of Mbouda. The small number of lineaments in the locality of Batang shows that the aquifer is difficult to recharge in this locality, which reduces the capacity of the boreholes located in the area to provide a high and permanent flow of water. The major directions of the lineaments in Batang that are N0-10° E and N160-170° E would be the work of a local tectonics affecting the basement (granito-gneissic) of Batang and could also be at the origin of the setting cracks in the basaltic parent rock.

4.5. Hydrogeological mapping

Interpretations of sounding curves, resistivities maps, electrical sections, interpretation of lineaments and their positions, and hydraulic parameters were used to establish a map of potential areas for water supply sites (Fig. 7), taking into account distribution curves at the bottom of the boat (H-

curves), the distribution of lineaments, the degree of fracturing of the rock present in the environment, piezometric curves and that hydraulic conductivity and the transmissivity of aquifers. This map identifies three potential areas: the wrong area in red, the right area in sky blue and the excellent area of implantation in ultra-blue.

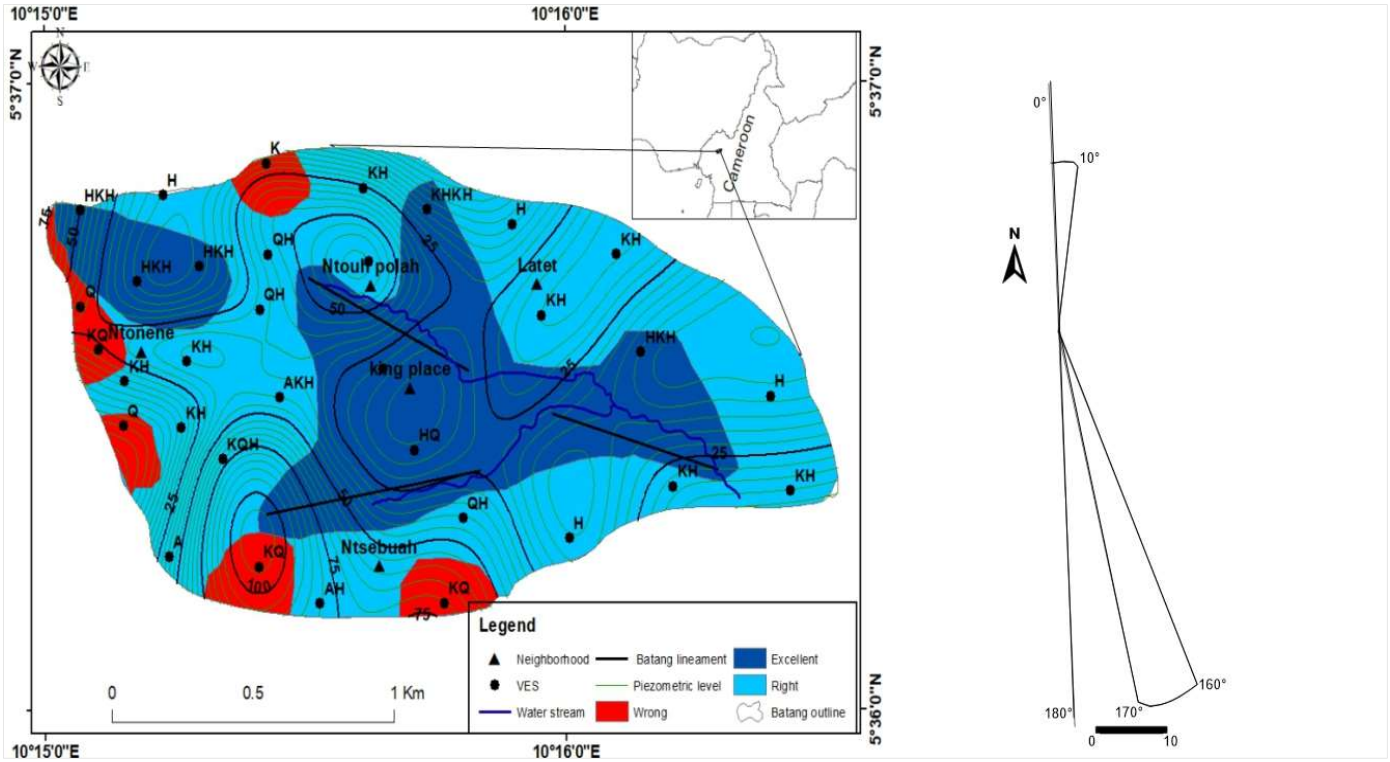

Fig. 7. Hydrogeological map of the study area and rose diagram

5. Discussion

It should be noted that, the values of the aquifer depths at certain positions seems very close to the ground surface but on the ground, no water table was observed and this could be due to the clay constituting the first layers of ground which by its non-permeability would prevent the contact of water with the free surface. It should also be noted that the observations made on the piezometers present on the ground show the aquifer level of the zone at enormous depths which seems to discredit the depths obtained by the empirical relation of Barker which would bring the level of the aquifer closer to the area. Actual values seem closer to those obtained using Boudoukha theory (Boudoukha, 2008).

The observation is that the studied area contains different aquifer systems in places, including a multilayer aquifer and a single-layer aquifer. The studied area therefore presents two main types of aquifers, the first with interstitial porosity (the table of otherness) identified in the lateritic formations which will be easily accessible using wells, the second with fracture permeability, located in fractured basalts and can only be accessed by drilling which would bring us closer to the results obtained by Boudoukha and Messaid (2014). The interstitial or otherness table is therefore superficial and would represent a free sheet while the fracture table is deep and represents a captive table. The very high resistivity values associated with clayey and lateritic materials and the poor superposition of the layers in the weathering profiles are due to the presence of small basalt blocks found throughout the study area and could be found at different levels of the profile associated with clays and laterites.

2D resistivity profiles present in the studied area resistance ranges that according to Hoareau (2009) would correspond to clays, laterites and certain levels to basalts. The hydrogeological characteristics of these different materials which include their ability to be crossed (permeability) allow recovering the results obtained by Sirhan and Hamidi (2012) to Hebron On the water infiltration road that would be related to material heterogeneity, cracks and porosity, which is probably interstice porosity. The hydrogeological lineaments in the major directional study area N0-170°E and N160-170°E would follow materialized cracks on basaltic mother rock and thus influence the hydrogeology and water dynamics of the locality. In accordance with the work of Rakoto et al. (2003) using a different method (remote sensing) contrary to the gravity method.

The lateral and vertical variations of the resistances, materialized on the iso-resistivity maps, would be the work of a global reshuffling of the different layers of terrain. This is due to the latest eruptions of the Bamboutos mountain very close to the studied area or the erosion phenomena that are repeated constantly in the locality because of its geomorphology. This variation would also be the work of differential alterations affecting basaltic rock materials in a heterogeneous manner evidence of environmental anisotropy. Depending on their mineral compositions, the

mineral variability of basalts could also create differential alterations within the basaltic rock matrix since depending on the hardness level of the different minerals, it can probably be inferred that some are easily more alterable than the others. This alteration must first leave porosity systems on the basaltic rock due to the disintegration of the olivine. These porosities would then be with the intensification of interconnected alteration (permeability) which could therefore allow water to pass through. They immediately become water cashing them in. This makes the rock become a water table that can hold water. It should also be noted that the quality of a water in terms of dissolved material depends on the mineral composition of the rock.

The waters of the study area would therefore be more mineralized in elements ca^{2+}, Fe^{2+}, Mg^{2+} ions from olivine, clinopyroxenes and plagioclase (basalt minerals). Indirectly, it is therefore possible to conclude on the turbidity of the aquifer. As for fracking processes, it all starts with the installation of micro-cracks within the basalts under the action of the point tectonics which is the origin of the formation of micro cracks in minerals with planes of weakness. This should in time become generalized on the whole of the rock to make room for cracks observable with the naked eye. These cracks therefore represent groundwater circulation networks.

Areas with low values of hydraulic conductivity would refer to clay aquifers on the ground because clays tend not to pass water by trapping it in their inter-sheet space. On the other hand, aquifers with high conductivity are those carried by the lateritic formations and the basaltic mother rock crack. These areas with large hydraulic conductivity are of great interest because the flow rate of the slick can be estimated from the values of hydraulic conductivity.

However, these areas also have great transmissions, therefore a very high-water potential and are therefore the most suitable places for the installation of water supply. It is therefore obvious that the recharge time of the water table has a high hydraulic conductivity is very short, i.e. to the north, center and east of the study area.

The hydrogeological map exposes three types of potential water supply implantation area. An excellent area, a right area and a bad area. It is then remarkable that the piezometric map has concentricity at or near excellent and good areas. This concentricity of isohypses generally marks the convergences or divergences of groundwater at a given location. It therefore individualizes piezometric depressions indicating punctuations in the water table by leaking water to an underlying aquifer and also piezometric domes corresponding to preferred infiltration surfaces.

In any case, the contribution of meteoric water to the study area, which is materialized by piezometric ridges and loss of resources leaving the study area to the surrounding areas by drainage, should not be overlooked. It therefore shows that areas proven to be excellent and good for the establishment of drinking water supply would be full of an underlying aquifer and would also be privileged areas of input by meteoric water infiltration.

6. Conclusion

Petrographic studies reveal that the area consists only of basalt which, in its matrix, has large olivine crystals that show alteration under a microscope and this at the macroscopic level reflects the presence of cracks through which the aquifer would circulate. Geophysical studies reveal two aquifer systems: a one-layer aquifer, marked on the map, by VES with a single boat bottom almost present throughout the study area, and a multilayer aquifer, due to the presence of alternating waterproof layers between two levels of aquifer superimposed locally in the environment and preventing the continuity of the phenomenon of weather water filtration at very great depths (present in the NORTH-West). Electrical cuts proof the existence of two types of aquifers: an alterian or interstitial aquifer circulating in laterite layers and a fracture aquifer circulating in the cracked part of basaltic bedrock. This cracking would be the result of tectonic efforts. The iso-resistivities maps reveal a lateral and vertical variation, evidence of the heterogeneity and anisotropy of the aquifer layer. As for the 2D sections, they indicate that the water table in places is the source of water in the water system. The directional rosette shows that Batang lineaments are due to local tectonics affecting the studied area. Nevertheless, the studied area has very few lineaments, which shows that the recharge time of the water table would be great and that these waters would have a high conductivity because of their long stay in the rock. Observations on piezometric curves are consistent with the spatial layout of potential areas obtained by superimposing VES, water systems and lineaments. Interpretation made on 1D sounding cuts allowed to calculate some hydraulic parameters. The values of these parameters suggest that the center, north and east of the studied area have aquifers very acceptable for exploitation.

References

Attwa, M, Basokur, A.T, Akca, I., 2014. Hydraulic conductivity estimation using direct current (DC) sounding data: a case study in East Nile Delta, Egypt. Hydrology Journal 22, 1163-1178.

Besse, A., 1996. Étude géophysique par méthode électrique à Maripasoula (Guyane). Rapport BRGM R39178, 17p.

Boudoukha, A., 2008. Identification des aquifères profonds par la prospection électrique application à l'est algérien. Science & Technologie A – N°28, Décembre. pp. 47-52.

Boudoukha, A., Messaid, B., 2014. Caractérisation électrique des formations aquifères de l'est algérien. Laboratoire de Recherche en Hydraulique Appliquée. Université Hadj Lakhadr. Batna. Courrier du Savoir – N°18 pp.77-82.

Castany, G., 1972. Terminologie hydrogéologique. Extrait de la chronique d'hydrogéologie (n°5 a 11,1965-1967) et du bulletin du BRGM, 139 p.

Daubree, A., 1887. Eaux souterraines à l'époque actuelle leur régime, leur température, leur composition au point de vue du rôle qui leur revient dans l'économie de l'écorce terrestre. Tome premier. Paris. vvech. dunod. 459p.

Deruelle, B., Moreau, C., Nkoumbou, C., Kambou, R., Lissson, J., Njonfang, E., Ghogomu, R.T., Nono, A., 1991. The Camaeroon Line: A Review. In: Kampunzu, A.B., Lubala, R.T. (eds) Magmatism in Extensional Structural Settings pp 274-327, Springer, Berlin, Heidelberg.

Desruelle, L., 2009. Hydraulique villageoise en zone d'aquifère de socle en Afrique de l'Ouest: analyse des données de forages.Master Gestion et Evaluation des Ressources en Eau.

Mémoire de stage de 2e année, Université Montpellier 2-DESTEEM. Département des Sciences de la Terre, de l'Eau et de l'Environnement, 75p.

Deruelle, B., 1982.Risques volcaniques au Mont Cameroun. Rev. Ecologie, Géog. Cameroun 3 (1), 33-40.

Dumort, J.C., 1968. Notice explicative sur la carte douala-ouest, direction des mines et de la geologie dessine par: c Espinasse BRGM société nouvelle de cartographie. lith. Paris

Heigold, P.C., Gilkeson, R.H., Cartwright, K., Reed, P.C., 1979. Aquifer transmissivity from surficial electrical methods. Gr Water 17, 338-345.

Hoareau, J., 2009. Utilisation d'une approche couplée hydrogéophysique pour l'étude des aquifères - Applications aux contextes de socle et côtier sableux. Thèse de Doctorat, Université Joseph Fourier (Grenoble I). 167p.

Kanohin, F., Saley, M.B., Ake, G.E., Savane, I., 2012. Apport de la télédétection et des SIG dans l'identification des ressources en eau souterraines dans la région de Daoukro (centre-est de la cote d'ivoire). International Journal of Innovation and Applied Studies 1 (1), 35-53.

Koussoubé, Y., Nakolendoussé, S., Bazié, P., Savadogo, A.N., 2003. Typologie des courbes de sondages électriques verticaux pour la reconnaissance des formations superficielles et leur incidence en hydrogéologie de socle cristallin du Burkina Faso. Sud Sciences & Technologies10, 26-32.

Marescot, L., 2004. Modélisation directe et inverse en prospection électrique sur les structures 3D complexes par la méthode des éléments finis. Génie civil. Universités de Nantes et de Lausanne.209p.

Marescot, L., 2006. Introduction à l'imagerie électrique du sous-sol. Bulletin de la Société Vaudoise des Sciences Naturelles 90 (1), 23-40.

Marescot, L., 2008. Imagerie électrique pour géologues: acquisition, traitement, Interprétation. Bulletin de la Société Vaudoise des Sciences Naturelles 90 (1) 73-78.

Marquis, G., 2005. Prospection électrique, EOST Strasbourg, 1-4, 6p.

Margat, J., 1990. Eaux souterraines dans le monde. BRMG, service sol et sous-sol département des eaux, 44p.

Morel, J., 2007. Les ressources en eau sur terre : origine utilisation et perspectives dans le contexte du changement climatique-un tour d'horizon de la littérature, halshs-0134979, 30p.

Morin, S., 1998. Les dissymétries fondamentales des hautes terres de l'ouest Cameroun, leur conséquence sur l'occupation humaine exemple des monts bambouto.in « l'homme et la montagne tropicale » éd.separit,bordeaux, pp35-56.

Niwas, S., Singhal, D.C., 1981. Estimation of aquifer transmissivity from Dar zarrouk parameters in porous media. Hydrology 50, 393-399.

Njueya, A.K., Likeng, J.D.H., Nono, A., 2012. Hydrodynamique et qualité des eaux souterraines dans le bassin sédimentaire de Douala (Cameroun): cas des aquifères sur formations Quaternaires et Tertiaires. International Journal Biological and Chemical Sciences 6 (4), 1874-1894.

Njueya, A.K., Kengni, L., Fonteh, F.M., Dongmo, K.A., Ntankouo, N.R., Nkouathio, A.G., Tazo, C., 2016. Apport des Sondages Électriques Verticaux à la Localisation et la Caractérisation des Aquifères en zone Volcanique au Cameroun: Cas d'Ebone et ses Environs. European Journal of Scientific Research 138 (1), 54-65.

Nono, A., Wabo, H., Youmbi, T.G., Ndekam, T.F.N., Biaya, S., Ekodeck, G.E., 2009. Influence de la nature lithologique et des structures géologiques sur la dynamique et la qualité des eaux souterraines dans les hauts plateaux de l'ouest - Cameroun : cas de la localité de Bandjoun. Africa Geoscience Review 16 (4), 281-298.

Nono, A., 2009. Influence de la nature lithologique et des structures géologiques sur la qualité et la dynamique des eaux souterraines dans les hauts plateaux de l'ouest-Cameroun 219, 222,223.

Nerouz, B., 2013. Détection de cavités par deux méthodes géophysiques: radar de sol et mesures de résistivités électriques. Thèse de doctorat. Sciences de la Terre. Université Paris Sud - Paris XI.154p.

Obiora, D.N, Ibuot, J.C, Alhassan, U.D, Okeke, F.N., 2018. Study of aquifer characteristic in Northern Paiko Niger State, Nigeria, using geoelectric resistivity method. International Journal of Environmental Science and Technology 15, 2423-2432.

Onema, 2010. Les eaux souterraines. Les agences de l'eau. Ministère de l'écologie du développement durable et de l'energie.8-fiche-eaux-souterraines-web, 4p.

Radstake, F., Chery, Y., 2009. Prospection géophysique pour la recherche de l'eau souterraine en Haïti. Hydrological Sciences Journal 37 (1), 1-12.

Rakoto, H., Andrieux, P., Ratsimbazafy, J-B., Llicoto, V., Rasolomanana, E., Pastor, L., Zuppi, G.M., 2003. La prospection gravimétrique dans la modélisation substratum sous formation sédimentaire: apport à l'hydrogéologie d'une zone semi-aride du sud de Madagascar. C.R. Géoscience 335, 335-363.

Unesco, 1997. Evaluation des ressources en eau. Manuel pour un examen des capacités nationales, 177p.

Unesco, 2003. Fait et chiffres: approvisionnement en eau et assainissement. http://www.unesco.org /année internationale de l'eau douce .html [consulté le 06 juin2018].

Union Africaine, 2012. Rapport de situation sur l'application des approches intégrées de la gestion des ressources en eau en Afrique .101p

Sirhan, A., Hamidi, M.O., 2012. Caractérisation des systèmes hydrogéologiques superficiels à Hebron (Cisjordanie, Palestine) en zone semi-aride par les méthodes géophysique électrique et électromagnétique. Compte Rendu Géoscience 344. 449-460.

Vicat, J.P., 1998. Esquisse géologique du Cameroun. Département des sciences de la terre, faculté des sciences, université de Yaoundé I, Cameroun et département des sciences de la terre université d'Orléans France, 9 p.

Yemmafouo, A., Ngouanet, C., Tepoule Ngueke, J.O., Kuete, M., 2009. Difficultés d'approvisionnement en eau potable de la ville de Mbouda (Ouest-Cameroun): une conséquence des changements d'utilisation du sol sur le bassin versant de la Tsé deng-Tamétap; approche multi source de télédétection. Université de dschang. Département de Geographie, 15p.